

# Measurement of the Diffractive Deep-Inelastic Scattering Cross Section with a Leading Proton at HERA

---

**Mikhail Kapishin (for the H1 Collaboration) \***

*JINR, Dubna, Russia*

*E-mail: kapishin@mail.desy.de*

Results are reported on a new measurement of the cross section for diffractive deep-inelastic scattering process  $ep \rightarrow eXp$  with the leading final state proton detected in the H1 Forward Proton Spectrometer, using data collected at HERA-2. The cross section dependences on the proton fractional longitudinal momentum loss  $x_p$  and the squared four-momentum transfer at the proton vertex are interpreted in terms of an effective pomeron trajectory and a sub-leading exchange. The hypothesis of proton vertex factorisation is tested. The ratio of the diffractive to the inclusive  $ep$  cross section is studied. The data are compared to QCD predictions at next-to-leading order based on parton distribution functions previously extracted from measurements of diffractive and inclusive deep-inelastic scattering.

*XVIII International Workshop on Deep-Inelastic Scattering and Related Subjects, DIS 2010*

*April 19-23, 2010*

*Firenze, Italy*

---

\*Speaker.

## 1. Introduction

Diffractive processes such as  $ep \rightarrow eXp$  have been studied extensively in deep-inelastic electron-proton scattering (DIS) at the HERA collider [1–4]. Their understanding at fundamental level is crucial for the development of quantum chromodynamics (QCD) at high parton densities. In a number of previous analyses, including [2], diffractive DIS events were selected on the basis of the presence of a large rapidity gap (LRG) between the leading proton and the remainder of the hadronic final state  $X$ . A complementary way to study diffractive processes is by direct measurement of the outgoing proton using Forward Proton Spectrometers (FPS) [1, 3]. In contrast to the LRG case, the squared four-momentum transfer at the proton vertex  $t$  can be reconstructed. The FPS also allows measurements up to higher values of the proton fractional longitudinal momentum loss  $x_P$  than is possible with the LRG method, extending into regions where the sub-leading trajectory is the dominant exchange. The FPS measurements provide a means of testing in detail whether the variables  $x_P$  and  $t$  associated with the proton vertex can be factorised from the variables  $\beta = x/x_P$  and  $Q^2$  describing the hard interaction with the photon. Here  $\beta$  is the longitudinal momentum fraction of the colour singlet carried by the struck quark,  $x$  is the Bjorken scaling variable.

## 2. The reduced cross section $\sigma_r^{D(4)}$ and test of proton vertex factorisation

In this report, a new measurement of the reduced cross section  $\sigma_r^{D(4)}(\beta, Q^2, x_P, t)$  for the diffractive DIS process  $ep \rightarrow eXp$  is presented, using the FPS data collected with the H1 detector at HERA-2. The reduced cross section is related to the diffractive structure functions  $F_2^{D(4)}$  and  $F_L^{D(4)}$  by

$$\sigma_r^{D(4)} = F_2^{D(4)} - \frac{y^2}{1+(1-y)^2} F_L^{D(4)},$$

where  $y$  is the inelasticity. The reduced cross section is equal to the diffractive structure function  $F_2^{D(4)}(\beta, Q^2, x_P, t)$  to good approximation in the relatively low  $y$  region covered by the current analysis. The analysed data sample corresponds to an integrated luminosity of  $156 \text{ pb}^{-1}$ . The data cover the range  $0.1 < |t| < 0.7 \text{ GeV}^2$ ,  $x_P < 0.1$ ,  $4 < Q^2 < 110 \text{ GeV}^2$  and  $0.001 < \beta < 1$ . The statistics of DIS

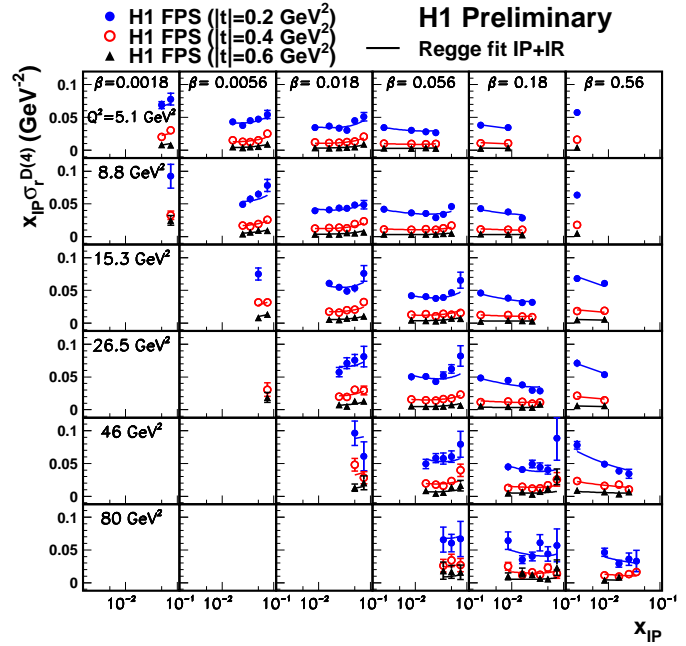


**Figure 1:** The diffractive reduced cross section, shown as a function of  $x_P$  for different values of  $t$ ,  $\beta$  and  $Q^2$ . The solid curves represent the results of the phenomenological ‘Regge’ fit to the data, including both pomeron ( $P$ ) and sub-leading ( $R$ ) trajectory exchange.

events with a leading proton are increased by a factor 20 compared to the previous H1 FPS analysis [1]. The kinematic range of the FPS measurement is extended to higher  $Q^2$ . Figure 1 shows  $x_P \sigma_r^{D(4)}$  as a function of  $x_P$  for different  $t$ ,  $\beta$  and  $Q^2$  values. To describe the  $x_P$  and  $t$  dependences quantitatively, the structure function  $F_2^{D(4)}$  is parameterised by the form

$$F_2^{D(4)} = f_P(x_P, t) \cdot F_P(\beta, Q^2) + n_R \cdot f_R(x_P, t) \cdot F_R(\beta, Q^2) ; \quad f_{P,R}(x_P, t) = A_{P,R} \cdot \frac{e^{B_{P,R}t}}{x_P^{2\alpha_{P,R}(t)-1}} ,$$

which assumes a separate proton vertex factorisation of the  $x_P$  and  $t$  dependences from those on  $\beta$  and  $Q^2$  for both the pomeron and a sub-leading exchange with no interference between the two contributions. The factors  $f_P$  and  $f_R$  correspond to flux factors for the exchanges and are taken from the Regge-motivated functions. The free parameters of the fit are the intercept and slope of the pomeron trajectory,  $\alpha_P(t) = \alpha_P(0) + \alpha'_P t$ , the exponential  $t$ -slope parameter  $B_P$ , the normalisation coefficients  $F_P(\beta, Q^2)$  for the pomeron contribution at each of the  $(\beta, Q^2)$  values considered, and the single parameter  $n_R$  describing the normalisation of the sub-leading exchange contribution. As in [1, 2], the normalisation coefficients  $F_R(\beta, Q^2)$  for the sub-leading exchange in each  $\beta$  and  $Q^2$  bin are taken from a parameterisation of the pion structure function [8].

The fit provides a good description of the  $x_P$  and  $t$  dependences of the data. The result for  $\alpha_P(0) \simeq 1.10$  (figure 2) is compatible with that obtained from H1 data previously measured using the LRG and FPS methods [1, 2] and with ZEUS measurements [3, 4]. It is also consistent within uncertainties with the pomeron intercept describing soft hadronic scattering,  $\alpha_P(0) \simeq 1.08$  [6].

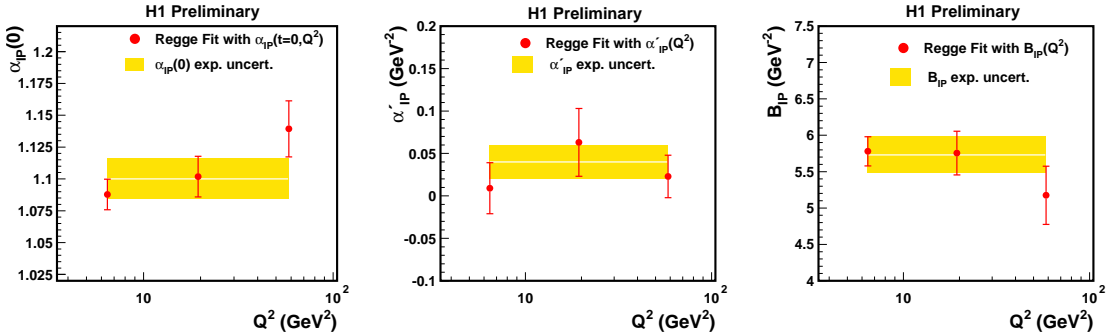


**Figure 2:** Results from the ‘Regge’ fit in which additional free parameters are included, corresponding to the values of  $\alpha_P(0)$ ,  $\alpha'_P$  and  $B_P$  in three different ranges of  $Q^2$ . The bands show the result and experimental uncertainty from the standard fit over the whole  $Q^2$  range.

In a Regge approach with a single linear exchanged pomeron trajectory,  $\alpha_P(t) = \alpha_P(0) + \alpha'_P t$ , the exponential  $t$ -slope parameter  $B$  of the diffractive cross section is expected to decrease logarithmically with increasing  $x_P$ , an effect which is often referred to as ‘shrinkage’ of the diffractive peak. The degree of shrinkage depends on the slope of the pomeron trajectory, which is  $\alpha'_P \simeq 0.25 \text{ GeV}^{-2}$  for soft hadron-hadron scattering at high energies. The FPS data favour a small value of  $\alpha'_P$  (figure 2), as expected in perturbative models of the pomeron [7]. This result is inconsistent with the expected value of  $\alpha'_P$  from soft hadron-hadron scattering. The results for  $\alpha'_P$  and  $B_P$  are compatible with those obtained previously from the H1 and ZEUS data measured using the FPS detectors [1, 3]. To check a possible breakdown of proton vertex factorisation implied by a dependence of the  $\alpha_P(0)$ ,  $\alpha'_P$  and  $B_P$  on  $Q^2$ , a modified version of the ‘Regge’ fit of the data is performed in

three different ranges of  $Q^2$ . The results of the fits, shown in figure 2, indicate no strong dependence on  $Q^2$ .

The  $t$ -dependence of the cross section is parameterised by an exponential function such that  $d\sigma/dt \propto e^{Bt}$ . Figure 3 shows the slope parameter  $B$  as a function of  $x_P$  for data averaged over  $Q^2$  and  $\beta$ . The results for  $B$  are compared with a parameterisation of the  $t$ -dependence from the ‘Regge’ fit to  $F_2^{D(4)}$ . A good description of the data over the full  $x_P$ ,  $Q^2$  and  $\beta$  range in figure 3 confirms the quality of the fit. At low  $x_P$ , the data are compatible with a constant slope parameter,  $B \simeq 6 \text{ GeV}^{-2}$ . No significant  $Q^2$  or  $\beta$  dependence of the slope parameter  $B$  is observed for data points with  $x_P \leq 0.025$ . The sub-leading exchange contribution integrated over this kinematic range is 7%. A weak decrease of the slope  $B$  from  $6 \text{ GeV}^{-2}$  to below  $5 \text{ GeV}^{-2}$  is observed towards larger values of  $x_P > 0.05$ , where the contribution from the sub-leading exchange is significant. This reduction of the slope parameter indicates that the size of the interaction region reduces for  $\mathbb{R}$  exchange compared to  $\mathbb{P}$ .

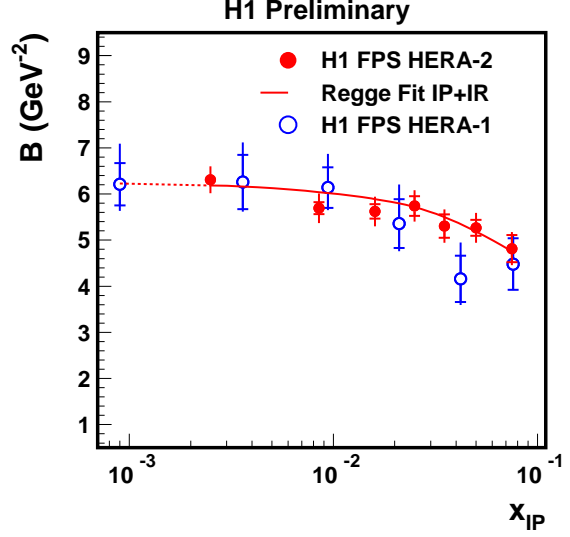


**Figure 3:** The slope parameter  $B$  obtained from the fit of the form  $d\sigma/dt \propto e^{Bt}$  shown as a function of  $x_P$ . The data are averaged over  $Q^2$  and  $\beta$ . The solid curve represents the results of the phenomenological ‘Regge’ fit to the data, including both pomeron ( $\mathbb{P}$ ) and sub-leading ( $\mathbb{R}$ ) trajectory exchange. The previously published H1 FPS results [1] are also shown.

### 3. Comparison between Diffractive and Inclusive DIS

By analogy with hadronic scattering, the diffractive and the total cross sections can be related via the generalisation of the optical theorem to virtual photon scattering [9]. Many models of low  $x$  DIS assume links between these quantities [10, 11]. Comparing the  $Q^2$  and  $x$  dynamics of the diffractive with the inclusive cross section is therefore a powerful means of developing our understanding of high energy QCD, comparing the properties of diffractive PDFs with their inclusive counterparts and testing models. Following [2], the evolution of the diffractive reduced cross section with  $Q^2$  is compared with that of the inclusive DIS reduced cross section  $\sigma_r$  by forming the ratio  $\sigma_r^{D(3)}(x_P, \beta, Q^2)/\sigma_r(x = \beta x_P, Q^2)$  multiplied by  $(1 - \beta)x_P$  at fixed  $Q^2, \beta$  and  $x_P$ , using a parameterisation of the  $\sigma_r$  data from [5]. The diffractive reduced cross section is integrated over  $|t| < 1 \text{ GeV}^2$ . The ratio of the diffractive to the inclusive cross section is indeed approximately constant with  $\beta$  at fixed  $Q^2$  except at large values of  $x_P$  where the sub-leading exchange contribution to the diffractive cross section is not negligible. In models in which both the diffractive and the inclusive cross sections are governed by a universal pomeron [10, 11], the remaining  $\beta$  and  $x_P$  dependences of the ratio arises due to the deviations from unity of the pomeron trajectory and the contribution of the sub-leading trajectory.

In order to compare the  $Q^2$  dependences of the diffractive and the inclusive cross sections quantitatively, the derivative of their ratio with  $\ln Q^2$  is extracted through fits of the form

$$(1 - \beta)x_P \sigma_r^{D(3)}(x_P, \beta, Q^2) / \sigma_r(x = \beta x_P, Q^2) = a_r(\beta, x_P) + b_r(\beta, x_P) \cdot \ln Q^2$$

The resulting values of  $b_r$  are shown in figure 4. The ratio of the diffractive to the inclusive cross section depends only weakly on  $Q^2$  for most  $\beta$  and  $x_P$  values (the logarithmic derivative of the ratio,  $b_r$ , is consistent with zero within  $1.5\sigma$  of the experimental uncertainties). Whereas the diffractive and inclusive reduced cross sections are closely related to their respective quark densities, the  $\ln Q^2$  derivatives are approximately proportional to the relevant gluon densities in regions where the  $Q^2$  evolution is dominated by the  $g \rightarrow \bar{q}q$  splitting. The compatibility of  $b_r$  with zero thus implies that the ratio of the quark to the gluon density is similar in the diffractive and inclusive cases when considered at the same low  $x$  values. Proton PDF predictions reproduce the behaviour of the  $\ln Q^2$  derivative of the ratio with  $\beta$ .

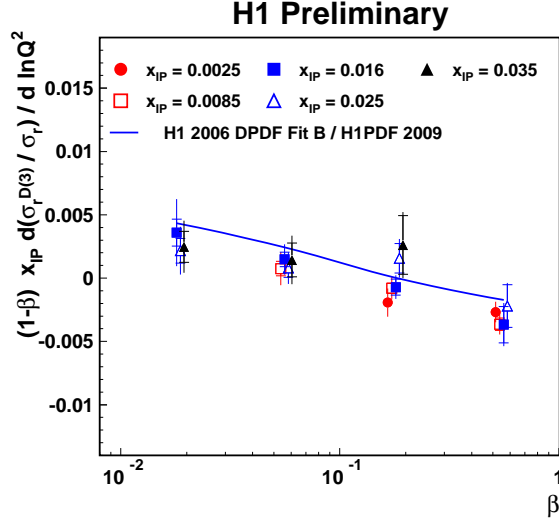


**Figure 4:** The logarithmic  $Q^2$  derivative of the ratio of the diffractive reduced cross section  $\sigma_r^{D(3)}(\beta, Q^2, x_P)$  to the inclusive reduced cross section  $\sigma_r(x = \beta x_P, Q^2)$  multiplied by  $(1 - \beta)x_P$ , shown at different fixed values of  $x_P$  and  $\beta$ . The solid curve represents the results for the ratio of diffractive to inclusive PDF predictions [2, 5].

## References

- [1] H1 Collaboration, Eur. Phys. J. C **48** (2006) 749
- [2] H1 Collaboration, Eur. Phys. J. C **48** (2006) 715
- [3] ZEUS Collaboration, Nucl. Phys. B **816** (2009) 1 [hep-ex/0408009].
- [4] ZEUS Collaboration, Nucl. Phys. B **800** (2008) 1
- [5] H1 Collaboration, Eur. Phys. J. C **64** (2009) 561 [arxiv:0904.3513]
- [6] G. Jaroszkiewicz and P. Landshoff, Phys. Rev. D **10** (1974) 170.
- [7] J. Bartels and H. Kowalski, Eur. Phys. J. C **19** (2001) 693 [hep-ph/0010345].
- [8] J. Owens, Phys. Rev. D **30** (1984) 943.
- [9] A. Mueller, Phys. Rev. D **2** (1970) 2963.
- [10] K. Golec-Biernat and M. Wüsthoff, Phys. Rev. D **59** (1999) 014017 [hep-ph/9807513].
- [11] J. Bartels, K. Golec-Biernat and H. Kowalski, Phys. Rev. D **66** (2002) 014001 [hep-ph/0203258].